*J. Phys. Chem. A* **2003,** *107,* 11223−11230

# Comprehensive Model for the Electronic Structures of 1,2,4-Cyclohexatriene and Related Compounds

**Patrick W. Musch, Daniel Scheidel, and Bernd Engels***

*Institut für Organische Chemie, Universität Würzburg, Am Hubland, D-97074 Würzburg, Germany*

*Received: October 7, 2003*

To gain a better understanding of the chemistry of cyclic allenes, in the present work six-membered monocyclic systems containing second- (B−O) and third-row elements (Al−S) of the periodic table of elements are studied in detail, regarding the energetic order of the electronic states and the planarization energies, which together determine their chemical behavior. The data obtained by high-level ab initio methods show that the properties of the compounds strongly depend on the heteroatoms and can be related to trends in the periodic table of elements. These trends in the series B to O and Al to S are rationalized by the degree of the interaction between the various fragments and the interplay between this interaction and the strain in the allene moiety. In addition, by applying the model to charged species, we reveal an unexpected link between the cyclic allenes and the phenyl anion. Furthermore, our computations answer open questions about the chemical properties of 1-aza-2,3-cyclohexadienes. Finally, we analyze how the various kinds of interaction influence the chemistry of this important class of intermediates.

## 1. Introduction

Trends in the periodic table of elements and the concepts related with them have become the foundation of current chemists thinking. Due to their simplicity and flexibility they represent powerful tools to explain variations in chemical structure and reactivity. However, quite often such trends are hidden behind the complexity of the properties and the structures of the various members belonging to a class of molecules. One example is the class of six-membered cyclic allenes represented in Scheme 1, which recently gathered much interest as intermediates in the cyclization of 1,3-diene-5-ynes,[1] the rearrangement of carbenes,[2−5] or as heterobenzene isomers.[6−8] Their complexity is expressed in the chemical properties that, being dependent on the fragment X, range from those of strained allenes (X = $CH_2$)[8−11] to those of zwitterionic systems (X = NH).[2,3,6] For X = O the chemical behavior varies between both extremes, depending on whether the six-membered ring or its benzo derivative is studied.[10,12] Systems with heteroatoms from the third row were also investigated to some extent. The role of a cyclic allene with X = S formed by rearrangement of a sulfur-substituted cyclopropylidene[13] was investigated by Shevlin et al.[4,5] Regitz et al. isolated a bulky substituted diphosphaisobenzene, which possesses substantial allene character.[7] This finding was supported by quantum chemical computations.[7] Taking into account the rather similar composition of the compounds, the variations in their chemical nature are unexpected.

As shown previously,[10,11] an explanation for the variations in the electronic structure can only be obtained, if, aside from the electronic structure at equilibrium geometry, also the electronic characters of the low-lying electronic states at planar geometry are included in the consideration. The orbital diagram from which these electronic states can be derived (see Scheme 1) is depicted in Scheme 2. The ring strain affects the allene moiety to that extent as it deviates from linearity and the bonding planes of the termini are arranged no longer perpendicular as in the parent allene $C_3H_4$.[13] For twisted ring geometries the character of an allene is maintained (Scheme 1, structure **a**). However, as is shown in Scheme 2, originally proposed by Johnson[16] for saturated ring systems, these geometric constraints lift the degeneracy of the $\pi$- and $\pi^*$-orbitals (depicted on the left-hand side of Scheme 2), and a set of 3 $\pi$-orbitals and 1 $\sigma$-orbital is obtained. The three lowest lying electronic states at planar geometry are obtained from the occupation pattern of

**SCHEME 1: Possible Electronic Structures of Cyclic Allenes (a−d)**[a]

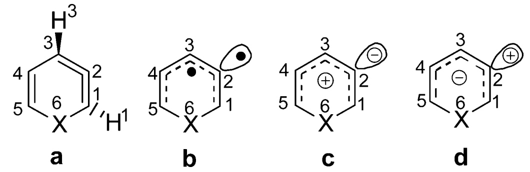

[a] The denotation of the planar zwitterionic species **c** and **d** will be used to reflect the reversed polarity compared to each other.

**SCHEME 2: Orbital Diagram for Strain-Induced Splitting of the Allene $\pi$-Orbitals[16]**

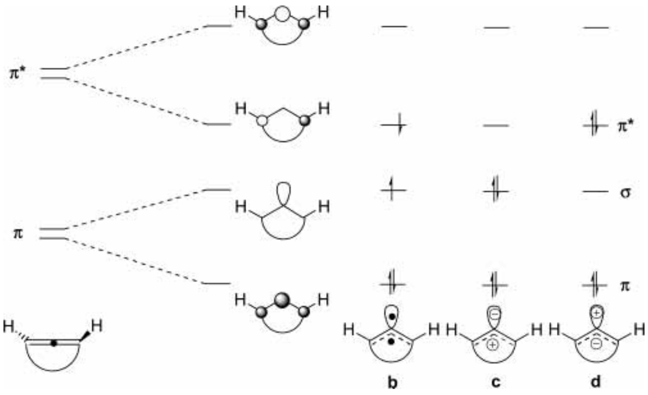

---

* To whom correspondence should be addressed. Fax: (+49) 931 8885331. E-mail: engels@chemie.uni-wuerzburg.de.

10.1021/jp037010h CCC: $25.00

these orbitals. The diradical state **b** originates from double occupation of the $\pi$-orbital and single occupation of the $\sigma$- and $\pi^*$-orbitals. Pairing of the latter two electrons in the $\sigma$-orbital leads to the zwitterion **c** possessing a formally negatively charged central carbon atom ($C^2$ depicted in Scheme 1) and a formal positive charge in the $\pi$-system of the allene moiety. In the following, all states with this formal charge distribution will be abbreviated as state **c**. If the occupation of the $\sigma$-orbital and the $\pi^*$-orbital of **c** is switched, a second zwitterion with reversed polarity (**d**) is obtained.

In the present paper, we extend the known considerations about the chemical nature of cyclic allenes by analyzing the variations within the series X = BH (**1**), $CH_2$ (**2**), NH (**3**), and O (**4**) and the series of the higher homologues with X = AlH (**5**), $SiH_2$ (**6**), PH (**7**,**8**), and S (**9**). With these data, which we obtained by high-level ab initio computations of the low-lying electronic states, we propose a comprehensive molecular orbital model in which the orbitals of the fragments (allenic unit, ethylene moiety, and fragment X) are successively combined to the orbitals of the entire system. This model fully explains the variations depending on the fragment X and shows their relationships to trends in the periodic table of elements. The model also reveals an unexpected connection between the class of cyclic allenes and the phenyl anion (X = $CH^-$). Finally, it is analyzed whether a model based on simple orbital energies actually contains all important aspects or if more subtle interactions also have to be considered (e.g., geometry relaxation, electron correlation).

## 2. Computational Aspects

For a reliable description of systems which possess diradical character, a multireference treatment is essential in most cases. Since the planar diradical species are significant for the understanding of the chemistry of cyclic allenes,[10,11,14,15] relative electronic energies of all species were computed at the multireference configuration interaction (MR-CI) and the CASPT2 level of theory employing (U)B3LYP geometries. Orbitals for the CASPT2 and MR-CI approaches were obtained by CASSCF calculations using the MOLCAS 5.0 package.[17] A balanced description of the active spaces in the CASSCF procedure chosen for the closed-shell compounds consisted of the two highest lying occupied $\pi$-orbitals (a″) with the corresponding number of virtual orbitals and the occupied $\sigma$-orbital (a′) at $C^2$. In addition, since the distorted geometries of the allenes possess $C_1$ symmetry, all $\sigma$-type orbitals lying between the $\sigma$-orbital at $C^2$ and the occupied $\pi$-orbitals were included. For the virtual orbitals a similar procedure was applied that include the $\sigma$-orbitals up to the unoccupied $\pi$-orbitals. The active space in the diradical species is merely identical to that of the closed-shell species except that the former lowest lying virtual $\pi$-orbital is now singly occupied to form the diradical and the number of virtual $\pi$-orbitals is reduced to one. This choice ensures that the allene includes the same $\pi$-orbitals in the active space as the planar species. With this ansatz [6,6] (X = $CH^-$, $NH_2^+$), [8,8] (X = BH, $BH^{2-}$, $CH_2$, NH, O, AlH, PH, S), and [10,10] (X = $SiH_2$, PH with additional P in the ring) CASSCF spaces resulted. For the diradical $^1A$ states of both phosphorus-containing compounds, the orbitals for the MR-CI computations were taken from the $^3A$ instead of a $^1A$ CASSCF calculation. This approximation was necessary since the relevant states **a** to **c** possess $C_1$ symmetry, and optimized orbitals for the $^1A$ state in the diradical **b** from excited-state CASSCF computations could not be obtained because of convergence problems. Test computations indicated that the use of these orbitals is appropriate, as the error in the MR-CI + Q computations employing optimized triplet orbitals instead of optimized singlet orbitals for the open-shell singlet wave function is within the expected error bar for this method of about 1−2 kcal $mol^{-1}$. All CASSCF and CASPT2 single-point computations were performed with the *MOLCAS 5.0* package.[17]

The MR-CI approach used in this study is based on a direct individually selecting MR-CI algorithm,[18] which computes the MR-CI energy for a reduced dimension of the CI eigenvalue problem, while the contributions of the neglected configuration state functions (CSF) were taken into account by the Buenker-Peyerimhoff extrapolation scheme.[19,20] The influence of quadruple excitations was estimated by the normalized form of the Davidson correction.[21] These calculations abbreviated as MR-CI+Q were performed with the DIESEL-CI program package.[22] The reference spaces of the individually selecting MR-CI computations were determined iteratively and consisted of up to nine reference configuration state functions, from which a configuration space of up to $47 \times 10^6$ CSF was generated. The number of secular equations to be solved in the reduced CI problem was up to the order of $12 \times 10^6$. The *ano-l*[23,24] basis set of triple-$\zeta$ quality in a 5s3p1d contraction for the atoms of the second and the third row and a 3s1p contraction scheme for hydrogen was used for all CASSCF, CASPT2, and MR-CI+Q calculations.

The reliability of the MR-CI+Q computations was checked against the energy differences between the cyclic allenes and the zwitterions (see Supporting Information) obtained at the CCSD(T) level of theory with the *MOLPRO* package.[25] For these computations the Dunning's *cc*-pVTZ[26] basis set with d-functions omitted for the hydrogen atoms was employed and is denoted as *cc*-pVTZ(f/p). The data of (U)B3LYP, CASPT2, MR-CI+Q, and CCSD(T) computations are provided in the Supporting Information. MR-CI+Q, CASPT2, and (U)B3LYP used in this work agree quite well on the energy separation of the states. The energy difference between the zwitterion and the allene **a** agrees well at the MR-CI+Q and CCSD(T) level of theory (max 2 kcal/mol, see Supporting Information). CASPT2 shows a slightly inferior performance, while it predicts comparable energies for the diradical states compared with MR-CI+Q. B3LYP does well for the zwitterionic and diradical states except for X = $CH_2$.

The geometric parameters of the stationary points were optimized by using analytical gradients of the density functional theory (DFT) utilizing the B3 exchange expression[27−29] in combination with the correlation functional by Lee, Yang, and Parr (LYP)[30] and Dunning's *cc*-pVDZ[26] basis set. This approach was found to give more appropriate geometries for a post Hartree−Fock treatment than the CASSCF method.[10,11] The singlet diradical species were optimized using broken-spin symmetry determinants in the unrestricted ansatz ($\langle S^2 \rangle$ approximately 1), while the planar and the nonplanar closed-shell species were computed within a restricted approach. The minima were optimized without symmetry constraints, while the geometries of the planar singlet species were determined in $C_s$ symmetry. If $C_1$ and $C_s$ optimized geometries were identical, the latter were used for the subsequent computations. The planar species of the phosphorus systems were optimized, constraining the dihedral angle of the allene moiety to 0° as the full $C_s$ symmetry could not be retained because of the $sp^3$ hybridized phosphorus center. The nature of the various stationary points was analyzed by calculation of the DFT harmonic frequencies. Vibrational analyses were also utilized at the (U)B3LYP level

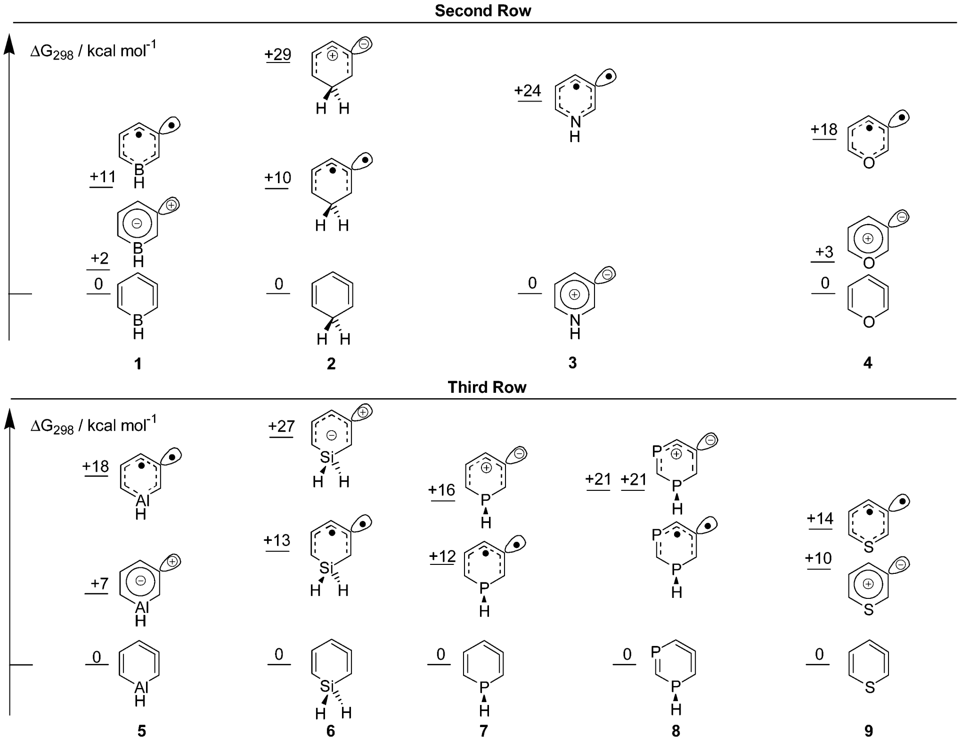

**Figure 1.** Energies and characters of the electronic states of 1,2,4-cyclohexatriene and its hetero analogues.

**TABLE 1: Geometric Parameters of Stationary Points**[a]

| | $d(C^1-C^2)$ | $d(C^2-C^3)$ | $d(X-C^1)$ | $d(X-C^5)$ | $\angle(C^1-C^2-C^3)$ | $\angle(H^1-C^1-C^3-H^3)$ |
|---|---|---|---|---|---|---|
| **1a** | 130 | 135 | 160 | 152 | 152 | 68 |
| **1b** | 136 | 140 | 157 | 156 | 128 | 0 |
| **1d** | 129 | 136 | 162 | 150 | 155 | 0 |
| **2a** | 133 | 134 | 152 | 153 | 131 | 100 |
| **2b** | 135 | 140 | 152 | 150 | 128 | 0 |
| **2c** | 140 | 143 | 149 | 148 | 110 | 0 |
| **3b** | 136 | 139 | 142 | 139 | 128 | 0 |
| **3c** | 140 | 142 | 137 | 135 | 111 | 0 |
| **4a** | 136 | 139 | 139 | 134 | 116 | 51 |
| **4b** | 135 | 139 | 140 | 138 | 127 | 0 |
| **4c** | 138 | 142 | 138 | 133 | 111 | 0 |
| **5a** | 130 | 134 | 201 | 194 | 158 | 89 |
| **5b** | 135 | 141 | 197 | 196 | 137 | 0 |
| **5d** | 127 | 136 | 209 | 190 | 162 | 0 |
| **6a** | 132 | 133 | 190 | 192 | 150 | 101 |
| **6b** | 135 | 140 | 189 | 188 | 134 | 0 |
| **6d** | 128 | 135 | 200 | 185 | 160 | 0 |
| **7a** | 132 | 133 | 185 | 184 | 144 | 94 |
| **7b** | 135 | 139 | 184 | 181 | 133 | 0 |
| **7c** | 134 | 140 | 185 | 175 | 130 | 0 |
| **8a** | 131 | 138 | 185 | 185 | 153 | 99 |
| **8b** | 135 | 139 | 183 | 180 | 138 | 0 |
| **8c** | 132 | 137 | 190 | 177 | 144 | 0 |
| **9a** | 134 | 135 | 178 | 176 | 132 | 83 |
| **9b** | 135 | 139 | 178 | 176 | 132 | 0 |
| **9c** | 139 | 142 | 177 | 170 | 115 | 0 |

[a] Distances are given in picometers and angles in degrees. The denotation of the species and the atomic centers can be taken from Figure 1 and Scheme 1.

to determine the thermal corrections to $\Delta G_{298}$. All DFT calculations were performed with the Gaussian 98 program package.[31]

## 3. Results

The influence of X on the electronic structure of the cyclic allenes of Scheme 1 can be taken from Figure 1, which summarizes the computed MR-CI+Q data of the present work.[32] Some geometric parameters are presented in Table 1. Figure 1 gives the energetic positions of the low-lying electronic states at planar ring geometry with respect to the allene structures which possess puckered ring geometries.[33] In addition to the parent compound 1,2,4-cyclohexatriene and systems with one heteroatom, we also studied the parent system of the known diphosphaisobenzene of Regitz[7] to evaluate the influence of the second phosphorus center in the ring system.

Figure 1 and Table 1 show that in the minimum[34] most compounds represent strained allenes with a more or less twisted ring geometry. The second lowest lying species (diradical or zwitterion) represents a transition state for the racemization of the allene. While most systems agree in this respect, the planarization energies strongly depend on the fragment X. For X = BH (**1**) and X = O (**4**) these energies are very small (2−3 kcal mol$^{-1}$), while it vanishes for the isopyridine **3** (X = NH), which hence prefers a zwitterionic ground state (**3c**, see Schemes 1 and 2) as equilibrium structure.[2−5,11] The planarization energy amounts 10 kcal mol$^{-1}$ for X = $CH_2$ (**2**). The planarization energies correlate with the dihedral angle of the allene moiety $H^1-C^1-C^3-H^3$, which is a measure for the distortion relative to an unstrained allene possessing a value of 90°. For X = $CH_2$ (**2a**), which possesses the largest planarization energy of the second-row systems, the dihedral angle (see Table 1) deviates from the optimum by only 10°. For X = BH (**1a**) and X = O (**4a**), which both possess a smaller barrier, this difference increases to 22° and 39°, respectively.

The planarization energy rises on going from second to third row fragments X, e.g., from X = BH (**1**) to X = AlH (**5**) from +2 to +10 kcal mol$^{-1}$. This increase in the energy difference is accompanied by a larger diameter of the six-membered monocycle containing third-row elements with respect to the second-row systems. The diameter rises according to Table 1, since the $X-C^1$ bond length increases, e.g., from 160 pm for X = BH (**1**) to 201 pm in X = AlH (**5**) and a similar change is obvious for the $X-C^5$ distance.

Aside from the planarization energies also the sequences of the electronic states at planar geometry depend on the fragment X. While the diradical state is favored over the zwitterionic one for **2**, **6**, and **7**, the reverse order is found for **1**, **3**, **4**, **5**, and **9**. The energy of the diradical and the zwitterionic state are not distinguishable for the phosphorus compound **8**. The additional phosphorus center in the ring (**8** vs **7**) destabilizes the diradical state by 9 kcal mol$^{-1}$, while the zwitterionic state is destabilized by 5 kcal mol$^{-1}$ with respect to the allene structure. The energy gaps between zwitterionic and diradical states range for second-row fragments X from 9 kcal mol$^{-1}$ in **1** to 24 kcal mol$^{-1}$ in **3**. No systematic variation in the gaps is found when the second- and the third-row systems are compared with each other. For instance, X = AlH (**5**) has a slightly larger energy gap (11 kcal mol$^{-1}$) than X = BH (**1**, 9 kcal mol$^{-1}$), but going from X = O (**4**) to X = S (**9**) the difference between the zwitterion and the diradical is reduced from 15 to 4 kcal mol$^{-1}$.

The situation is even more complex as the character of the zwitterionic states also depends on X. The electronic structure of the zwitterionic states of the oxygen (**4**) and the nitrogen (**3**) systems is characterized by a formally positively charged ring and a negatively charged central "allene" carbon atom (Scheme 1, electronic structure **c**).[10,11] For the zwitterionic state of X = $CH_2$ the same polarity was found.[10] Concerning X = BH (**1**) our computations predict a reversed polarity, which corresponds to the zwitterionic state **d** in Scheme 1. The opposite formal polarity of the zwitterions of **1** and **3** is nicely mirrored in the computed dipole moments (B3LYP level of theory). The dipole moment of **1d** is predicted to be 1.9 D with a direction that points through the molecular center toward $C^2$. This direction is in line with a formally negatively charged ring and a positively charged central "allene" carbon atom. The dipole moment of **3c** (5.5 D) points into the opposite direction and reflects the reverse polarity of the zwitterion (see Scheme 1). The polarity of the zwitterionic states of the second-row systems and that of their third-row homologues are the same, with an interesting exception found for X = $SiH_2$.

**SCHEME 3: Schematic Orbital Diagram Based on the Main Three Bond Moieties (Allene, Ethylene, and X)[a]**

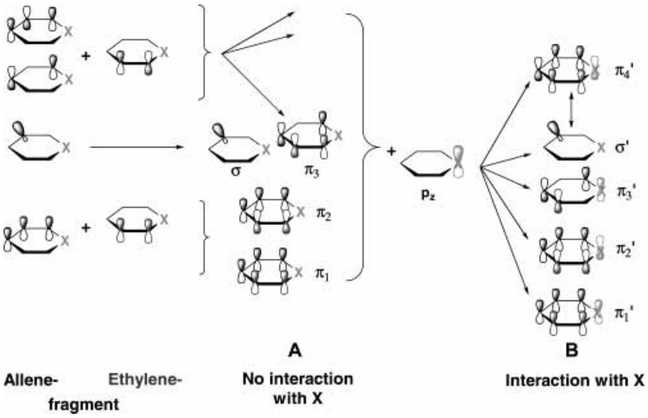

[a] The left-hand side (allene fragment) corresponds to Scheme 2.[16] Linear combination of the allene and the ethylene fragment extends the orbital scheme to set A in which fragment X has no contribution. Interaction of A with fragment X generates the orbital set B on the right-hand side.

In contrast to the geometric parameters of the allenes **a**, which correlate with the varying planarization energies, a similar relationship between the trends in the geometric parameters described above and the varying sequences of the planar states is not obvious (see Figure 1 and Table 1). As found for the allene structure as well as for the states at planar geometries the $X-C^1$ distances of the various compounds decrease systematically from B to O (e.g., 157 pm in **1b** to 140 pm in **4b**) and also from Al to S (e.g. 197 pm in **5b** to 178 pm in **9b**). The same sequences are found for the corresponding $X-C^5$ distance. While these parameters are expected to depend on X, all other parameters vary less with X but depend on the state under consideration. For the diradical states of all systems (second and third row) the $C^1-C^2$ and the $C^2-C^3$ distances are computed to be around 135 and 140 pm, respectively. In the zwitterionic states **c** these parameters are 138−140 pm ($C^1-C^2$) and 140−142 pm ($C^2-C^3$) with the exception of **7c** having considerably smaller $C^1-C^2$ distance of 134 pm and a $C^2-C^3$ bond length of 140 pm. The zwitterionic states **d**, which show a reversed polarity, possess bond lengths around 128 and 136 pm for $C^1-C^2$ and $C^2-C^3$, respectively. The most characteristic parameter to describe the structural differences between the zwitterionic states **c** and **d** and the diradical state **b** is the bond angle $C^1-C^2-C^3$ of the allene moiety. For all systems with fragments X from the second row, the $C^1-C^2-C^3$ angle of the zwitterionic state **c** is nearly constant around 111°, while the only zwitterionic state with reversed polarity (X = BH, **1d**) is predicted to be 155°. The diradical states **b** possess bond angles around 128°. A similar trend also exists for the third-row systems. The zwitterions **5d** and **6d** (X = AlH and $SiH_2$) possess similar bond angles $C^1-C^2-C^3$ of 160° and 162°, respectively, while for X = PH (**7c**) and X = S (**9c**) this angle is significantly smaller (130° for X = PH and 115° for X = S).

## 4. Discussion

A general model that explains the varying planarization energies and the sequence of the states at planar geometry can be obtained from an orbital diagram (Scheme 3) that builds up the molecular orbitals of the entire system at planar geometry from the orbitals of the fragments (allene moiety, ethylene unit, and fragment X). In analogy to Scheme 2, the orbitals of the allene form **a** can be obtained from the orbitals at planar geometry by relaxation to the lower molecular symmetry of the allene. The diagram starts from the orbitals of the allene moiety given by Johnson[16] (the left-hand side of Scheme 3, see also Scheme 2 for comparison), which are first combined with the $\pi$-orbitals of the ethylene fragment leading to orbital set **A**. The positive and negative linear combination of the bonding $\pi$-orbital of the allene fragment with the bonding $\pi$-orbital of the ethylene moiety yield two low-lying $\pi$-orbitals denoted as $\pi_1$ and $\pi_2$. In this model the nonbonding $\sigma$-orbital remains unchanged. The next $\pi$-orbital ($\pi_3$) arises from the linear combination of the nonbonding orbital of the allene fragment and the antibonding orbital of the ethylene moiety. Higher lying orbitals are not relevant for our problem. The combination of the orbitals of the allene and the ethylene moiety in Scheme 3 (orbital set A) is already sufficient to explain the properties of X = $CH_2$ (**2**), $SiH_2$ (**6**), and PH (**7**,**8**), as X cannot interact with the $\pi$-system. One bonding orbital of X = $CH_2$ or $SiH_2$ had the correct symmetry (negative linear combination of CH or SiH orbitals) but they represent C−H or Si−H $\sigma$-bonds which do not interact sufficiently with the $\pi$-system in orbital set A (Scheme 3). For X = PH no interaction of the lone pair of the phosphorus atom with the $\pi$-system occurs, since the $sp^3$ hybridization is energetically strongly favored over the $sp^2$ hybridization.

The relevant states for **2** and **6**−**8** arise from the occupation pattern of the $\sigma$-orbital and the $\pi_3$-orbital, which are quite close in energy. For the diradical species **b** (cf. Scheme 1) one electron occupies the $\pi_3$- and one the $\sigma$-orbital at the $C^2$ center. The two zwitterionic states with reversed polarity result if either the $\sigma$- (**c**) or the $\pi_3$-orbital (**d**) is doubly occupied. The polarities correspond to those of the states discussed by Johnson.[16] Within orbital set A the energy difference between **b** and **c** is mainly governed by the energy difference between the $\pi_3$- and the $\sigma$-orbital on one hand and the spin pairing energy on the other. Since $\pi_3$ and $\sigma$ are close in energy, the diradical state should be preferred relative to the zwitterion. For X = $CH_2$ (**2**) and PH (**7**,**8**) the $\sigma$-orbital is slightly lower in energy than the $\pi_3$-orbital so that the occupation pattern is $\sigma^2\pi_3^0$ and zwitterions of type **c** are found. Surprisingly, the electronic structure of the zwitterionic state of X = $SiH_2$ (**6**), which is about as high in energy as the zwitterionic state of the carbon system **2**, is described by the occupation pattern $\pi_3^2\sigma^0$ and consequently possesses a reversed polarity. In our opinion this finding is related to the silicon $\beta$-effect. It comprises hyperconjugation effects which stabilize a carboncationic center in the $\beta$-position to a silicon center.[35] Due to this effect, the zwitterionic state possessing an unoccupied $\sigma$-orbital is stabilized, since only this occupation pattern conserves a positively charged $C^2$ center in the $\beta$-position to the silicon center. Indeed, we find that for the lowest zwitterionic state of the Si system the above-mentioned hyperconjugation effects destabilize the $\sigma$-orbital with respect to the $\pi_3$-orbital to the extent that the energetic sequence of both is reversed and the latter gets doubly occupied while the former remains empty. It is interesting to note that this effect only arises for the zwitterionic state. In the diradical state both $\pi$- and $\sigma$-orbitals are energetically very close to each other but possess the sequence ($\sigma$ below $\pi$) as found in all other systems. A zwitterionic state with the normal occupation pattern ($\sigma^2\pi_3^0$) also exists for **6** but is much higher in energy ($\approx$54 kcal mol$^{-1}$ with respect to the allene form).

While the explanation of the trends for systems **2** and **6**−**8** is already possible utilizing orbital set A, it is not sufficient for the systems with X = BH, NH, O, AlH, and S, because their fragments X can interact due to their $p_z$-orbitals. The corresponding orbital scheme leading to orbital set B (right-hand side of Scheme 3) is an extension of the previously discussed set A and includes its interaction with the $p_z$-orbitals of the fragment X. The new $\pi$-system now possesses four $\pi$-orbitals that are relevant for our model. The orbitals $\pi_1'$, $\pi_2'$, and $\pi_3'$, which are constructed from linear combinations of the former $\pi_1$-, $\pi_2$-, and $\pi_3$-orbitals with the $p_z$-orbital, are stabilized with respect the latter and lie below the $\sigma$-orbital. Within a one-electron picture the $\sigma$-orbital is not affected. The next $\pi$-orbital ($\pi_4'$) is destabilized with respect to the former $\pi_3$, so that the energy gap to the $\sigma$-orbital is increased in comparison to the energy difference between the former $\pi_3$- and the $\sigma$-orbitals. The degree of interaction between the $\pi$-orbitals $\pi_1$, $\pi_2$, and $\pi_3$ and the $p_z$-orbital of X is relevant for the stabilization of $\pi_1'$, $\pi_2'$, and $\pi_3'$ and the destabilization of $\pi_4'$. As a consequence it determines the order of the electronic states at planar geometry. The degree of orbital interaction depends on the radial extension of the $p_z$-orbital as well as on its energy. These properties are mainly governed by the heteroatom in the fragment X and correlate with its electronegativity. The interplay between this interaction and the previously discussed strain in the allene moiety also determines the varying planarization energies.

The order of the electronic states at planar geometries is first addressed. For all systems with an appropriate $p_z$-orbital at the fragment X (**1**, **3**, **4**, **5**, **9**), the interaction between this $p_z$-orbital and the $\pi$ system of orbital set A leads to an energy gap between the $\sigma'$-orbital and the $\pi_4'$-orbital, which is larger than the gap between the former $\sigma$ and $\pi_3$. The larger gap favors a double occupation of the $\sigma$-orbital, so that the zwitterionic state is preferred with respect to the diradical one. The energy gap between both states is dominated by the degree of interaction. The interaction is strongest for X = NH, which also possesses the largest gap (24 kcal mol$^{-1}$) of all systems in Figure 1. The weaker interaction for X = O is expressed by a reduced gap of 15 kcal mol$^{-1}$, which is further reduced to 4 kcal mol$^{-1}$, if X = S is regarded. This finding is in line with the chemical experience about the $\pi$-donor capability of the heteroatoms. The fragments X = BH and AlH also possess $p_z$-orbitals which interact with the $\pi$-system of the carbon framework, so that the same orbital diagram, as has been described for X = NH, O, and S, is valid. However, the former systems differ from the latter ones as to the number of electrons. Due to their electron deficiency, B and Al both cannot contribute any electron to the $\pi$-system. Therefore only the six electrons contributed from the allene and the ethylene moiety are distributed among the three $\pi'$-orbitals and the $\sigma'$-orbital. Since the three $\pi'$-orbitals are lower in energy, they are occupied, while the $\sigma$-orbital stays empty. As a consequence the resulting zwitterionic state has the same polarity of the zwitterionic state **d** defined in Scheme 1. It has to be kept in mind that the reasons for the polarity (Scheme 1, doubly occupied $\pi^*$; here, empty $\pi^*$- and $\sigma$-orbital) are different.

The orbital occupation patterns also explain the geometric differences between the zwitterionic and diradical states. The bond angle $C^1-C^2-C^3$ was found to be the most characteristic parameter to describe the structural differences between the electronic states. The values in Table 1 in combination with the occupation pattern of the states show that this angle correlates with the occupation of the $\sigma$-orbital. For the zwitterionic states with a polarity as **c** (double occupation of $\sigma$) the angle is around 111°, while for zwitterionic states with a polarity like **d** (empty $\sigma$) the angle varies from 155° to 162°. For the diradical states **b** (singly occupied $\sigma$) it was computed to be around 128°. This shows that the angle depends on the spatial extent needed by the empty, the singly occupied, or the doubly occupied $\sigma$-orbital. This is in accordance with the VSEPR model.

To explain the planarization energy and the related electronic structure of the minimum, the stabilization effects resulting from the orbital interaction between the $p_z$-orbital of X and the $\pi$-system of orbital set A have to be compared with the opposing strain introduced in the allene moiety. In the planar structure the interaction between the various orbitals but also the strain in the allene moiety can be expected to have a maximum. On going to the allene structure, the strain decreases but also the strengths of the orbital interactions are expected to get smaller. So if the $p_z$-orbital and the $\pi$-system in A interact strongly, a planar structure arises, since the strain effects are overcompensated. If the orbital interactions are weaker the strain effects are dominant and a puckered ring results. The interplay between both effects determines the planarization energy. For X = NH (**3**) the degree of interaction in the zwitterion overcompensates the strain in the allene moiety and establishes the planar zwitterion as the minimum. The degree of interaction is reduced for X = O, because of the smaller $\pi$-donor capability of O with respect to N. As a result the stabilization of **c** is decreased with respect to X = NH and consequently the allene is slightly favored over the zwitterion.[10,11] For X = BH the planarization energy is similar to the value found for X = O. The question to what extent the different number of electrons of both systems influences the barrier will be addressed later.

The increase in the planarization energy on going from the second- to the third-row elements results from the larger diameter of the rings allowing a better release of the strain effects. A decreased interaction between the $3p_z$-orbitals of the third-row heteroatom X and the $\pi$-system in orbital set A could also be responsible for the higher planarization energy. A reduced interaction, however, would also lead to a smaller energy gap between the zwitterionic and the biradical states. The gap indeed decreases on going from X = O to S (15 kcal $mol^{-1}$ to 4 kcal $mol^{-1}$) but stays nearly constant if X = BH (9 kcal $mol^{-1}$) is compared to X = AlH (11 kcal $mol^{-1}$). Consequently, we expect that the increase in the planarization energy for both pairs results from somewhat more subtle causes.

The orbital diagram also explains the differences between the phosphorus containing systems **7** and **8**. The additional phosphorus center hampers the delocalization in the $\pi$-system of orbital set A, so that both, the diradical and the zwitterionic state, are destabilized with respect to the allene structure. This should also hold for other substitutions of the $C^4{-}H$ group since the carbon center enables an optimal delocalization.

The model based on the interplay between the strain in the allene moiety and the stabilization effects introduced by the orbital interaction of the fragment orbitals works very well for neutral species, so that the question arises whether it can also be extended to charged species. The computed values for three isoelectronic second-row systems (X = $BH^{2-}$, X = $CH^-$, X = $NH_2^+$), obtained with the MR-CI+Q approach, are summarized in Figure 2. Within our model the isobenzene (X = $CH_2$) and isopyridine (X = NH) systems are the two prototypes, since they are representatives for the different degrees of interactions and the resulting orbital schemes. Deprotonation of the first at the fragment X = $CH_2$ converts the isobenzene to the phenyl anion **2**$^-$ (X = $CH^-$).[36,37] In contrast to **2**, **2**$^-$ obviously possesses an occupied $p_z$-orbital that can perfectly conjugate with the $\pi$-system of orbital set A (see Scheme 3). Consequently, our orbital model predicts **2**$^-$ (X = $CH^-$) to possess a ground state that corresponds to the zwitterionic[38] state **c**. Its stabilization is expected to be even stronger with respect to the diradical state than that of **3** (X = NH). These predictions are confirmed by our MR-CI+Q computations, which result in a planar equilibrium geometry with a closed-shell electronic structure and a diradical state lying 47 kcal $mol^{-1}$ higher in energy than the ground state. This proves the distinctly stronger interaction in the $\pi$-system in comparison to **3** (X = NH), which possesses a gap of 24 kcal $mol^{-1}$. From the description it is obvious that **2**$^-$ behaves like **3** (X = NH) and not as its neutral precursor **2** (X = $CH_2$).

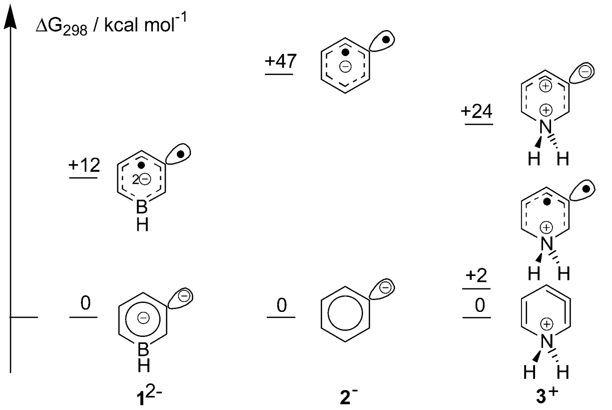

**Figure 2.** Order of the electronic states of the doubly negatively charged system **1**, the phenlyanion **2**$^-$, and the protonated isopyridine **3**$^+$.

Analogous to the change in the electronic structure of the pair **2**/**2**$^-$, protonation of isopyridine (**3**) to **3**$^+$ (X = $NH_2^+$) also leads to a change in the electronic structure. In this pair, the delocalization found in the $\pi$-system of **3** is destroyed due to the protonation. Indeed, our computations predict for X = $NH_2^+$ an allene species having a twisted ring as the equilibrium structure instead of the planar zwitterionic ground state, which is found for X = NH. The computed planarization energy is rather small (+2 kcal $mol^{-1}$), but at the planar structure the computations predict the diradical state to be preferred over the zwitterionic[38] one by 22 kcal·$mol^{-1}$, which is in difference to X = NH. This shows that the chemical nature of **3**$^+$ is very similar to that of **2** but distinctly different to that of **3**. This difference explains experimental findings from Christl et al., who found that a 1-aza-2,3-cyclohexadiene behaves completely different whether it has a three- or four-coordinated nitrogen atom.[39]

The doubly charged anion of **1**, **1**$^{2-}$ (X = $BH^{2-}$), is isoelectronic to **3**. Our MR-CI+Q computations predict that, in analogy to **3**, **1**$^{2-}$ possesses a planar equilibrium structure and a "zwitterionic"[38] ground-state only. The energy gap to the diradical state is much smaller than for X = NH. This may result from the stronger charge concentration in the ring. For the diradical state the charge is more distributed over the whole molecule.

Our qualitative model, which explains the varying planarization energy and the order of the electronic states at planar structure, is based on orbital energies, while the influence of the geometry, which varies considerably from state to state, and many-electron effects are not taken into account. The question arises to what extent these factors influence the picture. An answer to this question is given in Table 2, which depicts the energy differences between the zwitterionic and diradical states of X = $CH_2$, $CH^-$, NH, and O at various levels of theory. The levels of theory used reach from simple orbital considerations to the computed MR-CI+Q energies at optimized geometries. The latter were taken as reference (last line of Table 2).

**TABLE 2: Analysis of the Orbital, Geometric, and Many-Electron Contributions to the Energy Difference between b and c**[a]

| | $X = CH_2$ | $X = CH^-$ | $X = NH$ | $X = O$ |
|---|---|---|---|---|
| $\epsilon_{\pi}* - \epsilon_{\sigma}$[b] | +62 | +127 | +97 | +87 |
| $E^{det}_{\sigma\pi*}(\mathbf{c}) - E^{det}_{\sigma^2}(\mathbf{c})$[c] | −3 | +70 | +36 | +23 |
| $E^{det}_{\sigma\pi*}(\mathbf{b}) - E^{det}_{\sigma^2}(\mathbf{c})$[c] | −20 | +51 | +22 | +11 |
| $E^{CI}(\mathbf{b}) - E^{CI}(\mathbf{c})$ | −15 | +51 | +25 | +14 |

[a] All energy differences are given in kcal mol$^{-1}$. Geometries, which were taken for the calculation (diradical **b** and zwitterion **c**), are denoted in parentheses. Orbital energies were taken from CASSCF/cc-pVDZ computations. CI energies were obtained from MR-CI+Q/ano-l//(U)B3LYP/cc-pVDZ computations and energy expectation values were calculated with the DIESEL package[22] utilizing a cc-pVDZ basis set at (U)B3LYP/cc-pVDZ geometries. Note that the CI results in both basis sets are comparable. [b] Differences of orbital energies were computed with the orbitals of the 1A″ state at zwitterionic geometries. The corresponding orbital energy differences obtained for diradical geometries are 35 to 43 kcal mol$^{-1}$ lower in energy; i.e., all trends are kept. [c] $E^{det}$ corresponds to the energy expectation value of the main configuration state function (CSF) for each individual state. The main configuration for the zwitterionic state is $|...(19a''^2)(20a''^2)(21a'^2)\rangle$ and for the diradical state is $|...(19a''^2)(20a''^2)(21a'^1)(22a''^1)\rangle$. In $C_s$ symmetry the orbitals of the irreducible representation a′ correspond to $\sigma$-orbitals while those of a″ correspond to $\pi$-orbitals.

The first level, which can be used to estimate the energy differences between zwitterionic and diradical states, is based on the orbital energy differences ($\epsilon_{\pi}* - \epsilon_{\sigma}$). For $X = NH$ and $X = O$ this simple approach reproduces the correct order of the states but overestimates the energy differences substantially by a constant value of about 70 kcal mol$^{-1}$ ($X = NH$, 97 vs 25 kcal mol$^{-1}$ at the MR-CI+Q level of theory; $X = O$, 87 vs 14 kcal mol$^{-1}$). For $X = CH_2$ the correct order (diradical state below zwitterionic state) cannot be described since spin-pairing effects can only be considered if many electron effects are taken into account.

The term $E^{det}_{\sigma\pi*}(\mathbf{c}) - E^{det}_{\sigma^2}(\mathbf{c})$ includes many electron effects in a comparable manner as the Hartree−Fock approach[40] but neglects effects from geometry relaxation (equivalent to the vertical excitation energy). This level describes the order of the electronic states for $X = CH_2$ already correctly (−3 kcal mol$^{-1}$). For $X = NH$ and $X = O$ the computed differences between the diradical and the zwitterionic state are uniformly overestimated with respect to the MR-CI+Q values by only about 10 kcal mol$^{-1}$ (36 and 23 kcal mol$^{-1}$). If the geometric differences between the diradical state **b** and the zwitterionic state **c** are also considered, the relative energies $E^{det}_{\sigma\pi}{}^{*}(\mathbf{b}) - E^{det}_{\sigma}{}^{2}(\mathbf{c})$ deviate only by 3 to 5 kcal mol$^{-1}$ from the MR-CI+Q results, which also contain electron correlation effects. The small influence of the electron correlation effects is astonishing, since open-shell species are compared to closed-shell species.

## 5. Summary

Strained cyclic allenes containing heteroatoms of the second and third row exhibit strong variations in their chemical properties depending on the heteroatomic fragment. In this paper, we present a comprehensive model that explains all these variations, including the parent compound 1,2,4-cyclohexatriene. It is based on an orbital diagram in which the orbitals of the fragments (allene moiety, ethylene unit, and fragment X) are successively combined to build up the molecular orbitals of the entire system. The variations in the order of the electronic states and the planarization energy, which are both crucial for the reactivity of such compounds,[10,11] are explained by the interplay between the stabilization depending on the degree of orbital interaction and the strain effects in the allene moiety. The model is found to be valid for all experimentally known species and its predictions are in agreement with results obtained from MR-CI + Q computations, which were employed to characterize still unknown compounds. Apart from neutral species, the model is also applicable to charged systems. The consideration of **2**$^-$ ($X = CH^-$) reveals an unexpected relation between strained cyclic allenes and the phenyl anion. Comparing $X = NH$ with $X = NH_2^+$ the model also answers the open question why three- and four-coordinated 1-aza-2,3-cyclohexadiene and 1-aza-2,3,5-cyclohexatriene show different chemical reactivity. In addition, the present work investigates how the various factors (orbital energies, geometry relaxation, many electron, and correlation effects) influence the various properties. It is shown that orbital energy differences already describe all trends correctly. For quantitative predictions, the different geometries of the various states and the many electron effects are essential, while the remaining electron correlation is less important. This shows that qualitative predictions for an unknown species can be made if its orbital energies, which are already accessible by simple DFT calculations, are compared to the orbital energies of the system with $X = NH$. For quantitative predictions, however, more sophisticated approaches are necessary.

**Acknowledgment.** P. W. Musch thanks the Stiftung Stipendienfonds im Fonds der Chemischen Industrie for a graduate scholarship. We thank Prof. Dr. M. Christl and the members of Graduiertenkolleg 690 Electron Density: Theory and Experiment for valuable discussions.

**Supporting Information Available:** Absolute energies and computed structures of all stationary points in Cartesian coordinates (PDF). This material is available free of charge via the Internet at http://pub.acs.org.

## References and Notes

(1) Prall, M.; Krüger, A.; Schreiner, P. R.; Hopf, H. *Chem. Eur. J.* **2001**, *7*, 4386−4394.

(2) Pan, W.; Shevlin, P. B. *J. Am. Chem. Soc.* **1997**, *119*, 5091−5094.

(3) Emanuel, C. J.; Shevlin, P. B. *J. Am. Chem. Soc.* **1994**, *116*, 5991−5992.

(4) Pan, W.; Balci, M.; Shevlin, P. B. *J. Am. Chem. Soc.* **1997**, *119*, 5035−5036.

(5) McKee, M. L.; Shevlin, P. B.; Zottola, M. *J. Am. Chem. Soc.* **2001**, *123*, 9418−9425.

(6) Yavari, I.; Nourmohammadian, F.; Tahmassebi, D. *J. Mol. Struct.* **2001**, *542*, 199−206.

(7) Hofmann, M. A.; Bergsträ*β*er, U.; Rei*β*, G. J.; Nyulászi, L.; Regitz, M. *Angew. Chem.* **2000**, *112*, 1318−1320; *Angew. Chem., Int. Ed.* **2000**, *39*, 1261−1263.

(8) Christl, M.; Braun, M.; Mueller, G. *Angew. Chem.* **1992**, *104*, 471−472; *Angew. Chem., Int. Ed. Engl.* **1992**, *31*, 473−476.

(9) Christl, M.; Groetsch, S. *Eur. J. Org. Chem.* **2000**, 1871−1874.

(10) Engels, B.; Schöneboom, J. C.; Münster, A. F.; Groetsch, S.; Christl, M. *J. Am. Chem. Soc.* **2002**, *124*, 287−297.

(11) Schöneboom, J. C.; Groetsch, S.; Christl, M.; Engels, B. *Chem. Eur. J.* **2003**, *9*, 4641−4649.

(12) Christl, M.; Drinkuth, S. *Eur. J. Org. Chem.* **1998**, *237*, 7−241.

(13) The discussion of the ring opening of cyclopropylidene to allene and an overview on the quality of different theoretical levels to describe open-shell systems are given in selected references.[14,15]

(14) Bettinger, H. F.; Schreiner, P. R.; v. R. Schleyer, P.; Schaefer, H. F., III *J. Phys. Chem.* **1996**, *100*, 16 147−16 154.

(15) Bettinger, H. F.; v. R. Schleyer, P.; Schreiner, P. R.; Schaefer, H. F., III *J. Org. Chem.* **1997**, *62*, 9267−9275.

(16) The discussion of the orbital diagram for a bent planar allene fragment can be found in: Johnson, R. P. *Chem. Rev.* **1989**, *89*, 1111−1124.

(17) *MOLCAS Version 5*; Andersson, K.; Barysz, M.; Bernhardsson, A.; Blomberg, M. R. A.; Cooper, D. L.; Fleig, T.; Fülscher, M. P.; de Graf, C.; Hess, B. A.; Karlstöm, G.; Lindh, R.; Malmquist, P.-Å.; Neogrády, P.; Olsen, J.; Roos, B. O.; Sadlej, A. J.; Schütz, M.; Schimmelpfennig, B.;

Seijo, L.; Serrano-Andrés, L.; Siegbahn, P. E. M.; Stålring, J.; Thorsteinsson, T.; Veryazov, V.; Widmark, P.-O. Lund University: Sweden, 2000.

(18) Hanrath, M.; Engels, B. *Chem. Phys.* **1997**, *225*, 197−202.

(19) Buenker, R. J.; Peyerimhoff, S. D. *Theor. Chim. Acta* **1974**, *35*, 33−58.

(20) Buenker, R. J.; Peyerimhoff, S. D. *Theor. Chim. Acta* **1975**, *39*, 217−228.

(21) Langhoff, S. R.; Davidson, E. R. *Int. J. Quantum Chem.* **1974**, *8*, 61−72.

(22) *DIESEL-MR-CI*; Engels, B.; Hanrath, M. Universität Bonn: Germany, 1997.

(23) Widmark, P.-O.; Malmquist, P.-Å.; Roos, B. O. *Theor. Chim. Acta* **1990**, *77*, 291−306.

(24) Widmark, P.-O; Persson, B. J.; Roos, B. O. *Theor. Chim. Acta* **1991**, *79*, 419−432.

(25) *MOLPRO, a package of ab initio programs designed by H.-J. Werner and P. J Knowles, version 2002.1*; Amos, R. D.; Bernhardsson, A.; Berning, A. Celani, P.; Cooper, D. L.; Deegan, M. J. O.; Dobbyn, A. J.; Eckert, F.; Hampel, C.; Hetzer, G.; Knowles, P. J.; Korona, T.; Lindh, R. A.; Lloyd, W.; McNicholas, S. J.; Manby, F. R.; Meyer, W.; Mura, M. E.; Nicklass, A. Palmieri, P.; Pitzer, R.; Rauhut, G.; Schütz, M.; Schumann, U.; Stoll, H.; Stone, A. J.; Tarroni, R.; Thorsteinsson, T.; Werner, H.-J. 2002.

(26) Dunning, T. H., Jr. *J. Chem. Phys.* **1989**, *90*, 1007−1023.

(27) Becke, A. D. *Phys. Rev. A* **1988**, *38*, 3098−3100.

(28) Becke, A. D. *J. Chem. Phys.* **1993**, *98*, 1372−1377.

(29) Becke, A. D. *J. Chem. Phys.* **1993**, *98*, 5648−5652.

(30) Lee, C.; Yang, W.; Parr, R. G. *Phys. Rev. B.* **1988**, *37*, 785−789.

(31) Frisch, M. J.; Trucks, G. W.; Schlegel, H. B.; Scuseria, G. E.; Robb, M. A.; Cheeseman, J. R.; Zakrzewski, V. G.; Montgomery, J. A., Jr.; Stratmann, R. E.; Burant, J. C.; Dapprich, S.; Millam, J. M.; Daniels, A. D.; Kudin, K. N.; Strain, M. C.; Farkas, O.; Tomasi, J.; Barone, V.; Cossi, M.; Cammi, R.; Mennucci, B.; Pomelli, C.; Adamo, C.; Clifford, S.; Ochterski, J.; Petersson, G. A.; Ayala, P. Y.; Cui, Q., Morokuma, K.; Malick, D. K.; Rabuck, A. D.; Raghavachari, K.; Foresman, J. B.; Cioslowski, J.; Ortiz, J. V.; Baboul, A. G.; Stefanov, B. B.; Liu, G.; Liashenko, A.; Piskorz, P.; Komaromi, I.; Gomperts, R.; Martin, R. L.; Fox, D. J.; Keith, T.; Al-Laham, M. A.; Peng, C. Y.; Nanayakkara, A.; Gonzalez, C.; Challacombe, M.; Gill, P. M. W.; Johnson, B. G.; Chen, W.; Wong, M. W.; Andres, J. L.; Head-Gordon, M.; Replogle, E. S.; Pople, J. A. *Gaussian 98*, revision A.7; Gaussian, Inc.: Pittsburgh, PA, 1998.

(32) Note that the energies presented here deviate slightly (1 to 2 kcal·mol$^{-1}$) from previous publications[10,11] since the MR-CI+Q computations were redone to provide a more comparative and uniform basis for the discussion of all systems.

(33) See Supporting Information for further details.

(34) The term minimum is used in the context with reference to isomers that have the same connectivity as the structure of the cyclic allenes and represents a local rather than a global minimum on the potential energy surfaces in most cases considered. The global minima of the $C_6H_6$ and $C_5H_6N$ families, for example, to which **2** (X = $CH_2$) and **3** (X = NH) respectively belong, are surely the benzene and the pyridine.

(35) Lambert, J. B.; Zhao, Y.; Emblidge, R. W.; Salvador, L. A.; Liu, X.; So, J.-H.; Chelius, E. C. *Acc. Chem. Res.* **1999**, *32*, 183−190.

(36) Davico, G. E.; Bierbaum, V. M., DePuy, C. H.; Ellison, G. B.; Squires R. R. *J. Am. Chem. Soc.* **1995**, *117*, 2590−2599.

(37) Nicolaides, A.; Smith, D. M.; Jensen., F.; Radom, L. *J. Am. Chem. Soc.* **1997**, *119*, 8032−8088.

(38) In charged species the term zwitterion is not strictly defined. In the present study, this term is used for the states with an electronic structure that resembles the zwitterionic states of the neutral species (see also, Schemes 1 and 2).

(39) Drinkuth, S.; Groetsch, S.; Peters, E.-M.; Peters, K.; Christl, M. *Eur. J. Org. Chem.* **2001**, 2665−2670.

(40) This procedure is comparable to the restricted Hartree−Fock level, which includes many electron effects in an averaged manner.[41,42] The difference between the restricted Hartree−Fock ansatz and the present computation of $E^{\text{det}}$ is the orbitals. In this study orbitals are used that were optimized for the diradical state, while Hartree−Fock uses orbitals optimized for each state. The choice of the diradical orbitals is necessary to ensure a balanced description of both the $\sigma$-type orbital ($\sigma/\sigma'$) and the lowest unoccupied $\pi$-type orbital ($\pi_3/\pi_4'$).

(41) Jensen, F. *Introduction to Computational Chemistry*; John Wiley & Sons: Chichester, 1999; pp 59−64.

(42) Szabo, A.; Ostlund, N. S. *Modern Quantum Chemistry*; Dover Publications: Mineola, 1989; pp 39−107.